

## STELLAR PARAMETERS OF M DWARFS FROM LOW AND HIGH-RESOLUTION SPECTRA TOGETHER WITH NEW MODEL ATMOSPHERES

A. S. Rajpurohit<sup>1</sup>, C. Reylé<sup>1</sup>, M. Schultheis<sup>1</sup>, F. Allard<sup>2</sup>, R. Scholz<sup>3</sup> and D. Homeier<sup>2</sup>

**Abstract.** We present an optical spectral atlas of stars covering the whole M-dwarf sequence. It consists of 95 M dwarfs at solar metallicity observed at low-resolution with EMMI@NTT and 21 M-subdwarfs, extreme-subdwarfs and ultra-subdwarfs observed at high resolution with UVES@VLT. Using the most recent PHOENIX BT-Settl stellar model atmospheres we perform a detailed comparison with our observed spectra using  $\chi^2$  minimization technique. We confront the models with low-resolution spectra of M dwarfs at solar metallicity and we assign effective temperatures to the M dwarfs. We present temperature versus spectral type and colour relations and their comparison with others found in the literature. We also present our high-resolution spectra of the subdwarfs (sdM, esdM, usdM) and compare them to the newest grid of the BT Settl models which uses the revised solar abundances of Caffau et al (2011). This comparison allows us to study the spectral details of cool atmospheres, to determine precise [Fe/H] values for our objects, and to investigate the effect of metallicity on cool dwarf atmospheres. This study also helps to validate the atmosphere models and improve them by determining new constants on molecular opacities, dust cloud formation etc.

Keywords: stars: atmospheres, stars: fundamental parameters, stars: low-mass-brown dwarfs

### 1 Introduction

Low-mass stars ( $0.08M_{\odot}$  to  $0.6M_{\odot}$  depending on the metallicity) ,in particular M dwarfs, are the dominant stellar component of the Milky Way. They constitute 70% of all stars (Bochanski et al. 2010; Gould et al. 1996; Henry 1998) and nearly half (40%) of the total stellar mass of the galaxy. Our understanding of the Galaxy therefore relies upon the description of this faint component. Whereas subdwarfs (sdM, esdM, usdM) are among the faintest and coolest stellar objects. The locus of subdwarfs in the H-R diagram deviates from most of the field stars due to the metallicity difference that, that translates in different opacities compared to those of regular dwarfs. subdwarfs are sometimes called low metallicity halo stars or galactic thick disk stars based on their spectroscopic features, kinematics and ages. M dwarfs and subdwarfs have been employed in several Galactic studies as they carry the fundamental information regarding the stellar physics, Galactic structure, formation and dynamics. Thus the determination of accurate fundamental parameters for M dwarfs and subdwarfs has relevant implications for both stellar and Galactic astronomy. Because of their intrinsic faintness and a homogeneous sample with respect to age and metallicity has not yet been built. The energy distribution in M dwarfs and subdwarfs is governed by the presence of various molecular absorption bands such as TiO, VO and metal hydrides in the visual ( $\geq 4000$ ) to near-infrared ( $\leq 1.3\mu\text{m}$ ). However because of the decreasing metallicity for subdwarfs, the TiO bands are less strong, and the pseudo-continuum brighter as a result. But this increases the contrast to the other opacities such as hydride bands and atomic lines which feel the higher pressures of the deeper layers where they emerge from. We see therefore these molecular bands with more details than for M dwarfs and under more extreme gas pressure conditions. This often reveals the inaccuracy or incompleteness of the opacities used in the model. Thus the presence of these molecular bands reduces the strength of atomic lines and the spectral contrast. This makes the complexity of stellar atmosphere

<sup>1</sup> Observatoire de Sciences de l'Univers THETA de Franche-Comté, Université de Franche-Comté, Institut Utinam, UMR CNRS 6213, BP 1615, 25010 Besançon Cedex, France

<sup>2</sup> CRAL (UMR 5574 CNRS), École Normale Supérieure, 69364 Lyon Cedex 07, France

<sup>3</sup> Leibniz-Institut für Astrophysik Potsdam (AIP)

of subdwarfs increasing significantly with decreasing effective temperature. The effective temperature ( $T_{\text{eff}} < 4000$  K) and pressures in M dwarfs atmospheres allow for the widespread formation of the molecules. In dwarfs of spectral type later than M6 the outermost temperature falls below the condensation temperature of silicates which give rise to the formation of dust clouds (Tsuji et al. 1996b,a; Allard et al. 1997; Ruiz 1997; Allard et al. 1998). These processes complicate the understanding of these cool atmospheres. This means that the model atmosphere for low-mass stars has to take into account the formation of dust clouds and a variety of sometimes little studied molecules with large opacities, each affecting the abundance of the parent atomic population.

## 2 Model Atmosphere

In this study, we have used the recent new BT-Settl models (Allard et al. 2012) for our analysis of both low and high-resolution spectra. These model atmospheres are computed with the PHOENIX code using hydrostatic equilibrium, convection using the Mixing Length Theory and a mixing length of  $1/H_p=2.0$  according to results of radiation hydrodynamics (Ludwig et al. 2006), spherically symmetric radiative transfer, departure from LTE for all elements up to iron, the latest solar abundances by Asplund et al. (2009) and Caffau et al. (2011) equilibrium chemistry, an important database of the latest opacities and thermochemical data for atomic and molecular transitions, and monochromatic dust condensates refractory indexes. Grains are assumed spherical and non-porous, and their Rayleigh and Mie reflective and absorptive properties are considered. The diffusive properties of grains are treated based on 2-D radiation hydrodynamic simulations, including forsterite cloud formation to account for the feedback effects of cloud formation on the mixing properties of these atmospheres (Freytag et al. 2010). For this paper, we use the model grid described as follows:  $T_{\text{eff}}$  from 2000 K to 4000 K with 100 K step,  $\log g = 5.0$  dex, 5.5 dex,  $M/H = -2.0$  dex to +0.5 dex with 0.5 dex step<sup>i</sup>.

## 3 Comparison between atmosphere models with M-dwarf spectra

### 3.1 With low resolution EMMI@NTT

We compared 95 M dwarfs (from M0 to M9) low resolution spectra with optical spectroscopic classification (Reyl e et al. 2006) with the most recent PHOENIX stellar atmosphere model BT-Settl (Allard et al. 2012). Both theory and observation indicate the dwarfs having  $\log g = 5.0 \pm 0.2$  (Gizis 1996) and we therefore restrict our analysis to  $\log g = 5.0-5.5$  models. We have determined the  $T_{\text{eff}}$  by assuming solar metallicity for our low resolution sample. We confirmed the solar metallicity for all our objects by comparing them with isochrones at different metallicity (see Fig. 1) generated from BT-Settl model atmosphere. The fits of BT-Settl models to the low resolution spectra is shown in Fig. 2. The best fit spectra reproduce very well the TiO band which is very sensitive to temperature cooler than 4000 K as well as most of the spectral features, and also the overall shape of the optical to near IR spectra across the M dwarfs regime. The purpose of this fit was to determine the effective temperature by fitting the overall shape of the optical spectra which is dominated by molecular absorption. No attempt has been made to fit the individual atomic lines such as K I resonance doublet or Na I doublet for the low resolution spectra. Some discrepancies remain in the strength of some absorption bands such as the TiO absorption around 6500  , 7000  , CaH absorption around 6400  . The cause could be inaccurate atomic parameters and or missing molecular opacities.

### 3.2 With high resolution UVES@VLT spectra

We compared 21 high-resolution spectra of subdwarfs (sdM, esdM, usdM) with the most recent PHOENIX stellar atmosphere model BT-Settl. The TiO bands at 7053  , 7589  , 7666  , 8432  , and 8859   and VO bands at 7334  , 7851   and 8521   are very well recovered by the models and get weaker towards cooler temperature due to condensation into dust species like perovskite ( $\text{CaTiO}_3$ ), solid titanium oxide and vanadium oxides. The strongest atomic absorption lines in the spectra of usdM are the massively pressure broadened alkali lines, i.e. elements with only one electron in their outer shell, which can get excited even at very low temperatures. All alkali elements Ca I, Fe I, Ti I, K I, Na I have strong lines in the observed wavelength region. KI and Na I lines in early and mid M subdwarfs is well matched by the model but they become stronger and wide towards

<sup>i</sup><http://phoenix.ens-lyon.fr/simulator/index.faces>

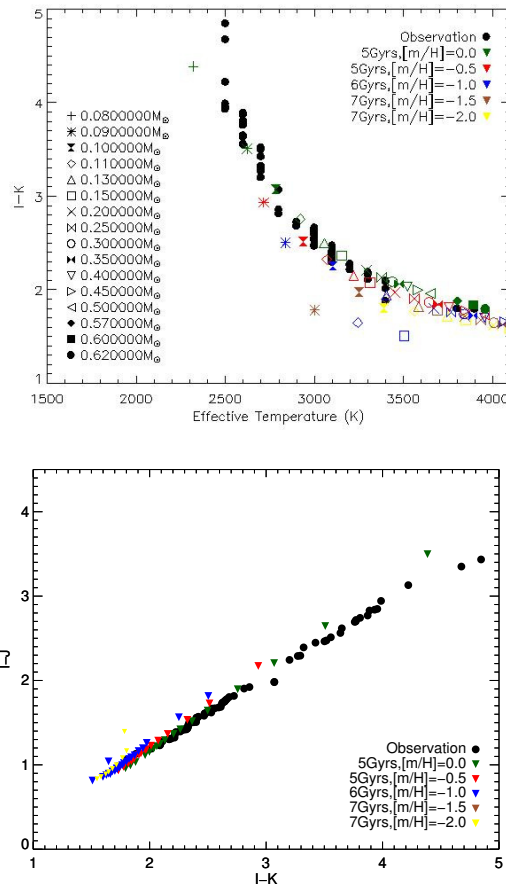


**Fig. 1.** Estimated  $T_{\text{eff}}$  and I-K color (**top panel**) and color-color plot (**bottom panel**) for observed M dwarfs (red) compared to the BT-Settl isochrones for 5,6 and 7 Gyrs (Baraffe et al. 1998) using BT-Settl model atmosphere.

lower temperature. The detailed analysis of these high-resolution spectra with the synthetic spectra will allow us to determine the metallicity of these subdwarfs and also helps to determine the strengths of molecular bands and atomic lines as well as damping constant of various features seen in these spectra. Figures 3 shows such comparison with the model atmosphere. The uncertainty from the fitting procedure are the grid spacing of 0.5 in [m/H] and 100 K in  $T_{\text{eff}}$ . Compared to Gizis (1996) our fits give somewhat 100K higher temperatures. The subdwarfs and extreme subdwarf have the best fit at [m/H]=−1.0 to [m/H]=−2.0.

#### 4 Effective temperature scale of M dwarfs

As photospheric temperatures decrease, atoms combine to form molecules; upon still further cooling, atoms and molecules may coagulate to form dust grains. Dust formation can change the atmospheric spectral characteristics in various ways. For example, grains can warm the photosphere by backwarming, making the spectral distribution redder while weakening molecular lines (example  $\text{H}_2\text{O}$  and  $\text{TiO}$ ) (Tsuji et al. 1996a). Dust formation decreases the photo-spheric gas phase abundance of the atoms that form dust (example Ti, Ca, Al, Mg, Si, Fe). Furthermore, with decreasing temperature, dust grains can become larger and gravitationally settle below the photosphere (Allard et al. 1998). Thus, in any attempt to assign effective temperatures to cool photospheres, we must make use of models that take dust formation and its behavior into account. The extreme temperature sensitivity of these metal oxide bands can be utilized for spectral classification and they are the primary temperature indicator of the cool stars.

The effective temperature is an important parameter to understand the cool atmosphere of low mass stellar and substellar objects. Many efforts have been made to derive a well secure effective temperature scale of M dwarfs but the scale is still uncertain because of the difficulty to accurately model the complex M dwarf spectra. The construction of  $T_{\text{eff}}$  sequences has been attempted in recent years by comparing the spectra of these objects

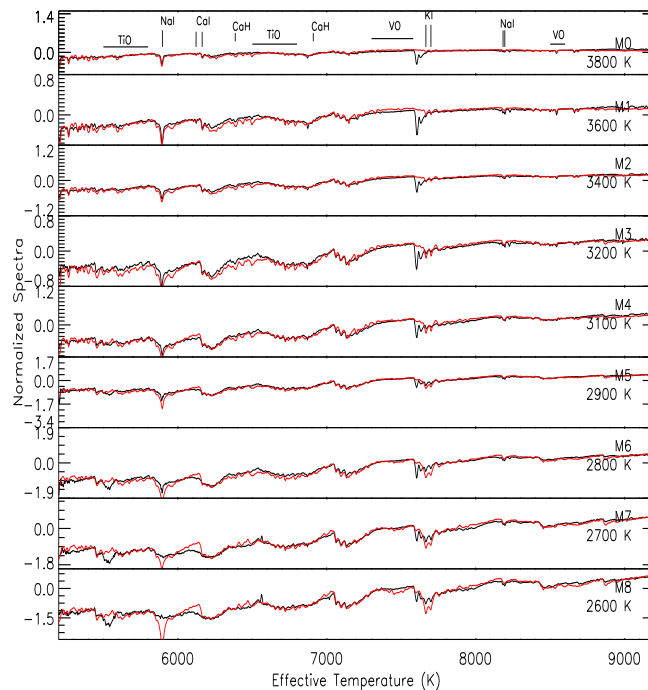


**Fig. 2.** Comparison of Observed spectral sequence of M dwarfs (black) with the best fit BT-Settl model (red). The main atomic and molecular features are indicated in the upper panel. The strong line at 7600 Å is telluric

to synthetic ones generated by atmospheric models (Reylé et al. 2011; Rajpurohit et al. 2011). In practice, the temperature derived from fitting to model spectra (Kirkpatrick et al. 1993) are systematically  $\sim 300$  K warmer than those estimated by empirical methods which is often wrong because they are based on using extrapolation of the Rayleigh jeans tails using historically the blackbody curve. Rajpurohit et al. (2011) and Reylé et al. (2011) used observed optical low resolution spectra to compare with the recent BT-Settl models which includes cloud physics and dust in it. Leggett et al. (1996) used observed infrared low resolution spectra and photometry to compare with NextGen models. They found radii and effective temperatures which are consistent with the estimates based on photometric data. Their study shows that these updated models should provide, for the first time, a realistic temperature scale of M dwarfs and subdwarfs. They found that the new model provides reasonable representations of the overall spectral features, with realistic strength variations induced by changes in stellar parameters. The adopted SpT (black) (figure 4) is the average from  $\text{TiO}_5$ ,  $\text{CaH}_2$  and  $\text{CaH}_3$  spectral indices. The relation is compared to others found in the literature

## 5 Conclusions

We have presented the effective temperature scale for the stars in our sample by comparing the observed spectra with synthetic spectra obtained with the most recent PHOENIX BT-Settl stellar model atmospheres (Allard et al. 2012). Our proposed effective temperature scale extended down to 2500 K where the dust and cloud in their atmosphere start forming. We found that the slope of the optical to near IR spectra is well reproduced by the models for both high and low resolution spectra, while some discrepancies remain in the strength of some absorption bands and atomic lines. The quality of the fit deteriorates as one goes from the early M to the late M. Our comparison to the observed spectra with most recent model atmosphere showed that the general features are understood and that probably most of the species and their spectral effects are taken into account. There are still improvements to be made in the models. There are important opacity sources for which laboratory data are needed such as oscillator strengths for hydrides for example. In extreme cool M dwarfs (esdM) and ultra-cool M dwarfs (usdM), it is necessary to achieve a very good fit to all the absorbers in order to determine atmospheric properties and to understand the effect of the chemical composition on their cool atmosphere.

We acknowledge financial support from Programme National de Physique Stellaire (PNPS) of CNRS/INSU, France.

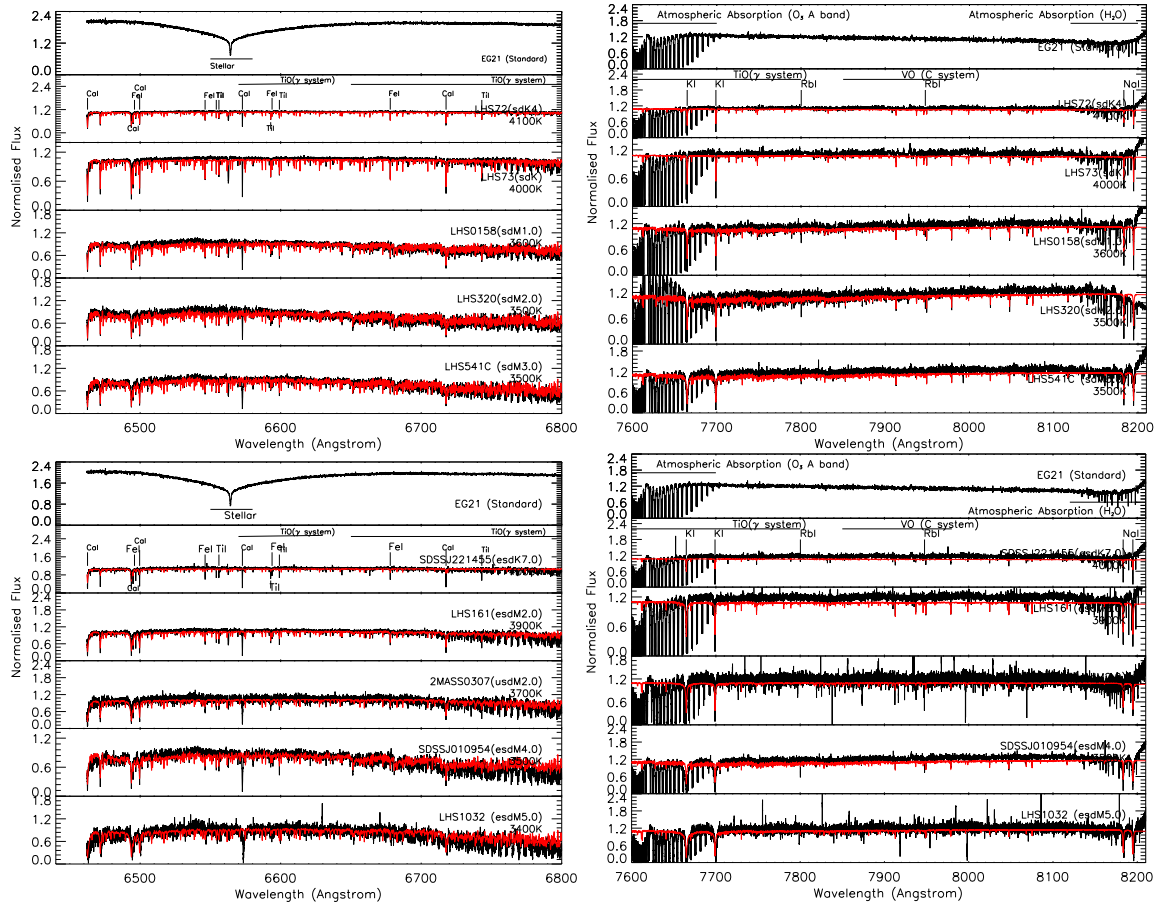


**Fig. 3.** Comparison of observed spectral sequence of sdM (**top**) and esdM (**bottom**) in black with the best fit BT-Settl model in red. The **left** and **right** panels show the different wavelength regime of UVES spectra.

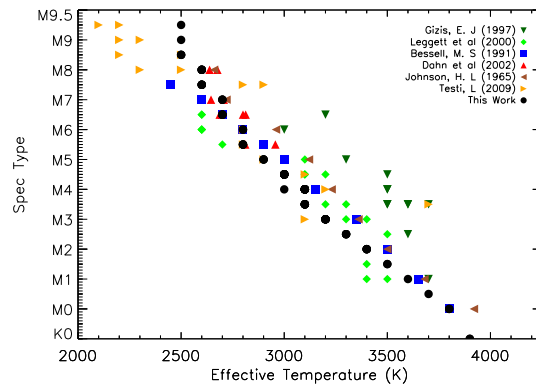


**Fig. 4.** Our adopted spectral type -  $T_{\text{eff}}$  relation (black) compared to relations from Leggett et al. (2001); Bessell (1991); Dahn et al. (2002).

## References

- Allard, F., Alexander, D. R., & Hauschildt, P. H. 1998, in *Astronomical Society of the Pacific Conference Series*, Vol. 154, *Cool Stars, Stellar Systems, and the Sun*, ed. R. A. Donahue & J. A. Bookbinder, 63
- Allard, F., Hauschildt, P. H., Alexander, D. R., & Starrfield, S. 1997, *ARA&A*, 35, 137
- Allard, F., Homeier, D., & Freytag, B. 2012, *Royal Society of London Philosophical Transactions Series A*, 370, 2765
- Asplund, M., Grevesse, N., Sauval, A. J., & Scott, P. 2009, *ARA&A*, 47, 481

- Baraffe, I., Chabrier, G., Allard, F., & Hauschildt, P. H. 1998, *A&A*, 337, 403
- Bessell, M. S. 1991, *AJ*, 101, 662
- Bochanski, J. J., Hawley, S. L., Covey, K. R., et al. 2010, *AJ*, 139, 2679
- Caffau, E., Ludwig, H.-G., Steffen, M., Freytag, B., & Bonifacio, P. 2011, *Sol. Phys.*, 268, 255
- Dahn, C. C., Harris, H. C., Vrba, F. J., et al. 2002, *AJ*, 124, 1170
- Freytag, B., Allard, F., Ludwig, H.-G., Homeier, D., & Steffen, M. 2010, *A&A*, 513, A19
- Gizis, J. E. 1996, in *Astronomical Society of the Pacific Conference Series*, Vol. 109, *Cool Stars, Stellar Systems, and the Sun*, ed. R. Pallavicini & A. K. Dupree, 683
- Gould, A., Bahcall, J. N., & Flynn, C. 1996, *ApJ*, 465, 759
- Henry, T. J. 1998, in *Astronomical Society of the Pacific Conference Series*, Vol. 134, *Brown Dwarfs and Extrasolar Planets*, ed. R. Rebolo, E. L. Martin, & M. R. Zapatero Osorio, 28
- Kirkpatrick, J. D., Kelly, D. M., Rieke, G. H., et al. 1993, *ApJ*, 402, 643
- Leggett, S. K., Allard, F., Berriman, G., Dahn, C. C., & Hauschildt, P. H. 1996, *ApJS*, 104, 117
- Leggett, S. K., Allard, F., Geballe, T. R., Hauschildt, P. H., & Schweitzer, A. 2001, *ApJ*, 548, 908
- Ludwig, H.-G., Allard, F., & Hauschildt, P. H. 2006, *A&A*, 459, 599
- Rajpurohit, A. S., Reyl , C., Schultheis, M., Leinert, C., & Allard, F. 2011, in *SF2A-2011: Proceedings of the Annual meeting of the French Society of Astronomy and Astrophysics*, ed. G. Alecian, K. Belkacem, R. Samadi, & D. Valls-Gabaud, 339–343
- Reyl , C., Rajpurohit, A. S., Schultheis, M., & Allard, F. 2011, in *Astronomical Society of the Pacific Conference Series*, Vol. 448, *16th Cambridge Workshop on Cool Stars, Stellar Systems, and the Sun*, ed. C. Johns-Krull, M. K. Browning, & A. A. West, 929
- Reyl , C., Scholz, R.-D., Schultheis, M., Robin, A. C., & Irwin, M. 2006, *MNRAS*, 373, 705
- Ruiz, J. 1997, *Earth Moon and Planets*, 77, 99
- Tsuji, T., Ohnaka, K., & Aoki, W. 1996a, *A&A*, 305, L1
- Tsuji, T., Ohnaka, K., Aoki, W., & Nakajima, T. 1996b, *A&A*, 308, L29